

Bonding along a Linear B···N···B Triad

Peter D. Livant,* D. John D. Northcott, Yiping Shen, and Thomas R. Webb

Department of Chemistry, Auburn University, Auburn, Alabama 36849-5312

livanpd@auburn.edu

Received May 17, 2004

The synthesis of tris(2,6-dihydroxyphenyl)amine diborate, **4**, is reported. This compound contains a linear B···N···B array for which a symmetrical three-center two-electron (3c-2e) bond is possible. The X-ray crystal structure of **4** shows that 3c-2e bonding is, in fact, absent. Rather, the B–N–B array of **4** is unsymmetrical, having a 2c-2e B–N dative bond with the remaining boron pyramidalized outward and bonded to the oxygen of THF, i.e., **4**·THF. In THF solution, **4** displays temperature-dependent ¹³C NMR spectra from which a ΔG^\ddagger of 11.6 kcal/mol at 262 K may be calculated. The dynamic process observed in solution corresponds to a bond-switching equilibrium in which the B–N bond oscillates between the two borons (“bell clapper”). Ab initio calculations indicate that the most likely pathway for the bond switch does not involve a 3c-2e B···N···B bond, but rather occurs by nucleophilic attack of THF on the datively bonded boron to generate **4**·(THF)₂, lacking any B–N interactions, followed by loss of one THF. The B–N–B system of **4** sans the perturbing effect of solvent was also investigated computationally. The form of **4** containing a 3c-2e bond is found to be a transition state in the solvent-free bond-switch reaction of **4**, lying 2.66 kcal/mol above **4**. The stability of three-center bonds to in-line distortion (viz., X···Y···X → X–Y···X) is discussed from the point of view of the second-order Jahn–Teller effect.

The syntheses decades ago of the noble gas halides¹ provided the impetus for extending and modifying then-current ideas about bonding. The conceptual advance called for was provided by Pimentel,² and Hach and Rundle,³ who proposed the three-center four-electron (3c-4e) bond to explain bonding in interhalogen anions (e.g., ICl₂[−]) as well as in the noble gas halides.⁴ The usual orbital diagram of a 3c-4e bond is shown in Figure 1 for a linear X–Y–X triad.

The 3c-4e bond concept has a history of 50 years of success in rationalizing and predicting the chemistry of so-called hypervalent⁵ systems, yet it is still, for some, an object of skeptical scrutiny.⁶ Until fairly recently, all known hypervalent systems had central atoms which were nonmetals found in the third row of the periodic

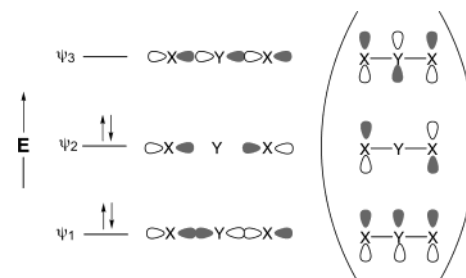


FIGURE 1. An MO picture of a 3c-4e bond in the X–Y–X array. In parentheses, for comparison, is a diagram of the analogous π -allyl system.

table and beyond—e.g., SF₆, PhI(OAc)₂, etc.—with the exception of the bifluoride ion, FHF[−], a unique case of hypervalency in the first row.⁷ Chemists had come to believe hypervalency in elements of the second row was highly improbable. However, the seminal work of Martin and later Akiba, and others, has recently provided startling examples of hypervalency in the second-row elements, to wit, in boron,⁸ carbon,⁹ and fluorine.¹⁰ An isolable example of nitrogen hypervalency (10-N-5) has

(7) *Chemistry of Hypervalent Compounds*; Akiba, K.-y., Ed.; Wiley-VCH: New York, 1999.

(8) (a) Lee, D. Y.; Martin, J. C. *J. Am. Chem. Soc.* **1984**, *106*, 5745–5746. (b) Yamashita, M.; Yamamoto, Y.; Akiba, K.-y.; Nagase, S. *Angew. Chem., Int. Ed.* **2000**, *39*, 4055–4058.

(9) (a) Forbus, T. R., Jr.; Martin, J. C. *J. Am. Chem. Soc.* **1979**, *101*, 5057–5059. (b) Forbus, T. R., Jr.; Martin, J. C. *Heteroat. Chem.* **1993**, *4*, 113–128. (c) Forbus, T. R., Jr.; Martin, J. C. *Ibid.* **1993**, *4*, 129–136. (d) Forbus, T. R., Jr.; Martin, J. C. *Ibid.* **1993**, *4*, 137–143. (e) Akiba, K.-y.; Yamashita, M.; Yamamoto, Y.; Nagase, S. *J. Am. Chem. Soc.* **1999**, *121*, 10644–10645.

* To whom correspondence should be addressed.

(1) Laszlo, P.; Schrobilgen, G. *J. Angew. Chem., Int. Ed. Engl.* **1988**, *27*, 479–489.

(2) Pimentel, G. C. *J. Chem. Phys.* **1951**, *19*, 446–448.

(3) Hach, R. J.; Rundle, R. E. *J. Am. Chem. Soc.* **1951**, *73*, 4321–4324.

(4) Rundle, R. E. *J. Am. Chem. Soc.* **1963**, *85*, 112–113.

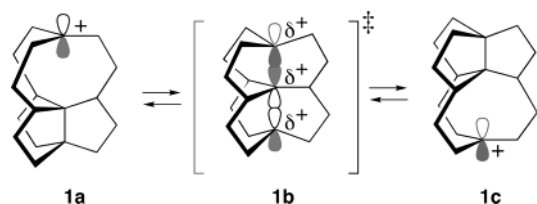
(5) We adopt here the Musher definition of this term. (a) Musher, J. I. *Angew. Chem., Int. Ed. Engl.* **1969**, *8*, 54–68. (b) Schleyer, P. v. R. *Chem. Eng. News* **1984**, May 28, 4. (c) Martin, J. C. *Ibid.* **1984**, May 28, 4. (d) Harcourt, R. D. *Ibid.* **1985**, Jan 21, 3.

(6) (a) Kutzelnigg, W. *Angew. Chem., Int. Ed. Engl.* **1984**, *23*, 272–295. (b) Mayer, I. *J. Mol. Struct.: THEOCHEM* **1987**, *149*, 81–89. (c) Mayer, I. *Ibid.* **1989**, *186*, 43–52. (d) Kar, T.; Marcos, E. S. *Chem. Phys. Lett.* **1992**, *192*, 14–20. (e) Häser, M. *J. Am. Chem. Soc.* **1996**, *118*, 7311–7325. (f) Harcourt, R. D. *J. Phys. Chem. A* **1999**, *103*, 4293–4297. (g) Sannigrahi, A. B.; Kar, T. *J. Mol. Struct.: THEOCHEM* **2000**, *496*, 1–17. (h) Molina, J. M.; Dobado, J. A. *Theor. Chem. Acc.* **2001**, *105*, 328–337. (i) Ponec, R.; Roithová, J. *Ibid.* 383–392. (j) Papoian, G.; Hoffmann, R. *J. Am. Chem. Soc.* **2001**, *123*, 6600–6608. (k) Ienco, A.; Hoffmann, R.; Papoian, G. *Ibid.* 2317–2325. (l) Papoian, G.; Hoffmann, R. *J. Solid State Chem.* **1998**, *139*, 8–21.

not yet been achieved, although attempts have been reported sporadically since 1916.¹¹ Transient 9-N-4 species have been observed by ESR¹² and by neutralization–reionization mass spectrometry.¹³ Theorists have pondered hypothetical hypervalent nitrogen species¹⁴ and other second-row hypervalent systems.^{6d,15}

If one is to succeed in preparing a 10-N-5 species, it is reasonable to guess that (i) the geometry about 10-N-5 nitrogen will be trigonal bipyramidal and (ii) the five ligands around nitrogen will have to be held in place. Indeed, Christie et al. have pointed out that fitting five fluorines about a central nitrogen may be impossible.¹⁶ Therefore, we sought to design a suitable scaffolding to hold in place a possibly recalcitrant three-center bond having nitrogen as the central element.

In Figure 1, the node structure of the orbitals involved in a three-center bond can be seen to correspond with that of an ordinary allyl system, in which three p orbitals interact in a π fashion. Because of this, the three-center bond is sometimes termed a “ σ -allyl” system. Baldrige, Leahy, and Siegel (BLS)¹⁷ calculated that a proposed all-carbon σ -allyl cation, **1b**, with a symmetrical 3c-2e bond, was not a global minimum, but rather a transition structure connecting ordinary carbocations **1a** and **1c**.



Transition structure **1b** was found to be 14.1 kcal/mol higher in energy than **1a/1c** using DFT (B3PW91/

(10) (a) Cahill, P. A.; Dykstra, C. E.; Martin, J. C. *J. Am. Chem. Soc.* **1985**, *107*, 6359. (b) Ault, B. S.; Andrews, L. *Inorg. Chem.* **1977**, *16*, 2024. (c) Hunt, R. D.; Thompson, C.; Hassanzadeh, P.; Andrews, L. *Inorg. Chem.* **1994**, *33*, 388–391. (d) Tuinman, A. A.; Gakh, A. A.; Hinde, R. J.; Compton, R. N. *J. Am. Chem. Soc.* **1999**, *121*, 8397–8398.

(11) (a) Schlenk, W.; Holtz, J. *Chem. Ber.* **1916**, *49*, 603. (b) Schlenk, W.; Holtz, J. *Ibid.* **1917**, *50*, 274, 276. (c) Wittig, G.; Wetterling, M. *Liebigs Ann. Chem.* **1947**, *557*, 193. (d) Hellwinkel, D.; Seifert, H. *Ibid.* **1972**, *762*, 29. (e) Olah, G. A.; Donovan, D. J.; Shen, J.; Klopman, G. *J. Am. Chem. Soc.* **1975**, *97*, 3559. (f) Johnson, R. W.; Holm, E. R. *Ibid.* **1977**, *99*, 8077. (g) Christie, K. O.; Wilson, W. W.; Schrobilgen, G. J.; Chirakal, R. V.; Olah, G. A. *Inorg. Chem.* **1988**, *27*, 789–790.

(12) (a) Nishikida, K.; Williams, F. *J. Am. Chem. Soc.* **1975**, *97*, 7166. (b) Hasegawa, A.; Hudson, R. L.; Kikuchi, O.; Nishikida, K.; Williams, F. *Ibid.* **1981**, *103*, 3436.

(13) (a) Shaffer, S. A.; Sadilek, M.; Turecek, F. *J. Org. Chem.* **1996**, *61*, 5234–5245. (b) Fuke, K.; Takasu, R. *Bull. Chem. Soc. Jpn.* **1995**, *68*, 3309–3318. (c) Nguyen, V. Q.; Sadilek, M.; Ferrier, J.; Frank, A. J.; Turecek, F. *J. Phys. Chem. A* **1997**, *97*, 6621–6627. (d) Nguyen, V. Q.; Sadilek, M.; Ferrier, J.; Frank, A. J.; Turecek, F. *J. Phys. Chem.* **1997**, *101*, 3789–3799.

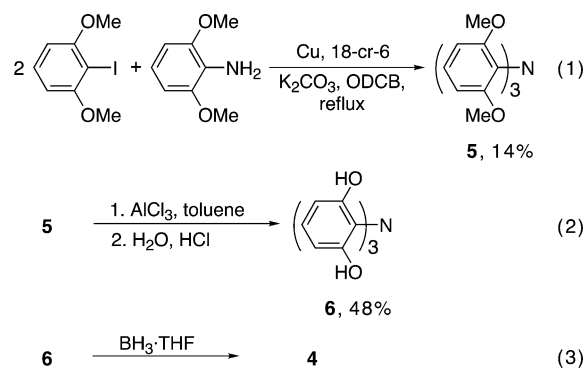
(14) (a) Bettinger, H. F.; Schleyer, P. v. R.; Schaefer, H. F., III. *J. Am. Chem. Soc.* **1998**, *120*, 11439–11448. (b) Boldyrev, A. I.; Simons, J. *J. Chem. Phys.* **1992**, *97*, 6621–6627. (c) Ewig, C. S.; Van Wazer, J. R. *Ibid.* **1990**, *112*, 109–114. (d) Ewig, C. S.; Van Wazer, J. R. *Chem. Eng. News* **1990**, April 2, p. 3. (e) Ewig, C. S.; Van Wazer, J. R. *J. Am. Chem. Soc.* **1989**, *111*, 4172–4178. (f) Morosi, G.; Simonetta, M. *Chem. Phys. Lett.* **1977**, *47*, 396–398. (g) Murrell, J. N.; Scollary, C. E. *J. Chem. Soc., Dalton Trans.* **1976**, 818–822. (h) Keil, F.; Kutzelnigg, W. *Ibid.* **1975**, *97*, 3623–3632.

(15) (a) Harcourt, R. D. *Int. J. Quantum Chem.* **1996**, *60*, 553–566. (b) Vetter, R.; Zülicke, L. *Chem. Phys.* **1986**, *101*, 201–209. (c) Dedieu, A.; Veillard, A. *J. Am. Chem. Soc.* **1972**, *94*, 6730–6738.

(16) Christie, K. O.; Wilson, W. W.; Schrobilgen, G. J.; Chirakal, R. V.; Olah, G. A. *Inorg. Chem.* **1988**, *27*, 789–790.

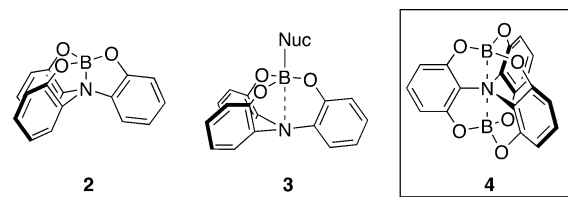
(17) Baldrige, K. K.; Leahy, J.; Siegel, J. S. *Tetrahedron Lett.* **1999**, *40*, 3503–3506.

SCHEME 1



cc-pvdz) calculations. BLS noted that in cases which lacked the polycyclic framework of **1** (e.g., $[\text{CMe}_3\cdots\text{CMe}_3\cdots\text{CMe}_3]^+$) the symmetrical 3c-2e structure analogous to **1b** was much more unfavorable energetically, or was a higher order stationary point. Therefore, in their words, **1** “comes a long way toward the desired effect” of stabilizing the delocalized σ -allyl cation (i.e., the 3c-2e bond).

Reactions of **2** with nucleophiles would lead to **3**, in which a pentacoordinate boron (10-B-5) might be present. This system was explored in detail by Müller and Bürgi.¹⁸ Our interest in hypercoordinate (if not hypervalent) nitrogen led us to mate **3** with **1** and generate thereby target structure **4**. This structure would accommodate,



and perhaps enforce, a trigonal bipyramidal geometry at nitrogen. At the very least, it would ensure that the two borons and nitrogen would be collinear. A symmetrical B–N–B triad in **4** would be evidence of a 3c-2e bond, analogous to that in **1b**. If that were the case, the conversion of the 3c-2e bond of **4** to a 3c-4e system would be worth exploring as a way of synthesizing a 10-N-5 species. Although this goal has not yet been reached, we report herein our synthesis of **4** and studies of the nature of bonding along its B–N–B axis.

Results and Discussion

The outline of our synthesis of **4** is shown in Scheme 1. The Ullmann reaction of 2,6-dimethoxyiodobenzene with 2,6-dimethoxyaniline (eq 1) was reported by Jackson et al.¹⁹ to give **5** in 9% yield. We modified the procedure somewhat and obtained a 14% yield of **5**. We found, as Jackson et al. had reported, that prolonged reaction times resulted in the formation of cyclized product **7**. Extending that result, we found that prolonged heating of **7** under the reaction conditions gave more highly cyclized products, which we have identified spectroscopically as **8** and

(18) (a) Müller, E.; Bürgi, H.-B. *Helv. Chim. Acta* **1987**, *70*, 499–510. (b) *Ibid.* 511–519. (c) *Ibid.* 520–533. (d) *Ibid.* 1063–1069.

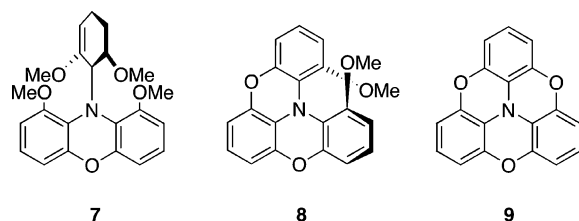
(19) Stoudt, S. J.; Gopalan, P.; Kahr, B.; Jackson, J. E. *Struct. Chem.* **1994**, *5*, 335–340.

TABLE 1. ^{13}C NMR Chemical Shifts (ppm) of **6**, **10**, and **4**^a

	C1	C2, C6	C3, C5	C4
hexaphenol 6	123.6	157.2	108.2	124.8
monoborate 10	126.0	151.9, 159.5	106.0, 111.9	131.0
diborate 4	124.6	154.3, 160.0	108.9	129.4

^a THF-*d*₈ solvent; the aromatic carbon bearing N is defined as C1.

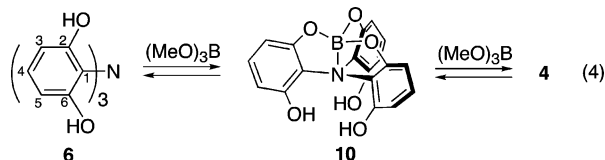
9. Conditions which reproducibly lead to useful yields of the intriguing structures **8** and **9** have eluded us,



unfortunately. Curiously, the material to which we assign the structure **9** on the basis of its FAB mass spectrum (base peak = m/z 287 = MW of **9**) gave no peaks in its ^1H NMR spectrum.

Demethylation of **5** with AlCl_3 (eq 2) was based on the procedure used by Frye et al.²⁰ in their synthesis of tris-(2-hydroxyphenyl)amine. The product amine hexaphenol **6** crystallized as $\mathbf{6}\cdot(\text{EtOAc})_2$ from EtOAc/hexane. The X-ray crystal structure of $\mathbf{6}\cdot(\text{EtOAc})_2$ revealed the geometry about nitrogen was perfectly planar (sum of C–N–C angles 360.0°) as was the case with the parent hexamethoxyamine **5**.¹⁹ Both compounds have 2-fold rather than 3-fold symmetry with the crystallographic C_2 axis coincident with one N–C bond. In **5**, the differences between the unique phenyl ring and the other two are slight (twist angles 62.0° , 61.0° , and 61.0°), but in $\mathbf{6}\cdot(\text{EtOAc})_2$ the differences are more pronounced (twist angles $70.3(1)^\circ$, $61.7(2)^\circ$, and $61.7(2)^\circ$). We were encouraged that the nitrogen of **6** was planar since a trigonal bipyramidal nitrogen (either 3c-2e or 3c-4e) would require the equatorial substituents to lie in a plane containing the nitrogen.

Several methods were tried to convert **6** to the target **4**. Reaction of **6** with tris(dimethylamino)borane produced an intractable solid. Reaction of **6** with trimethyl borate (THF-*d*₈ solvent, 65°C , 1.5 h) gave an equilibrium mixture of **6**, monoborate **10**, and the desired diborate **4** as shown in eq 4. The progress of this reaction was



followed most conveniently by ^{13}C NMR. The ^{13}C spectra of **6**, **10**, and **4** are summarized in Table 1. We noticed in the ^{13}C NMR spectrum of **4** that C3 and C5 were equivalent, indicating that **4** had “top/bottom” symmetry

(20) Frye, C. L.; Vincent, G. A.; Hauschildt, G. L. *J. Am. Chem. Soc.* **1966**, *88*, 2727.

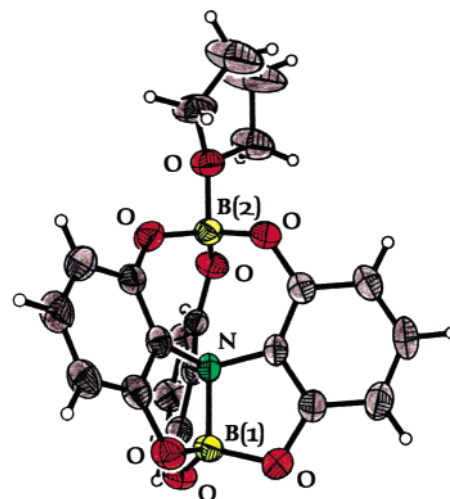


FIGURE 2. ORTEP plot of **4**. Nitrogen is depicted in green, boron in yellow, oxygen in orange, and carbon in gray. Hydrogens are depicted by open circles.

(as in **6**), but C2 and C6 were nonequivalent, indicating that **4** lacked top/bottom symmetry, as in **10**—a small mystery.

Finally, it was found that reaction of **6** with $\text{BH}_3\cdot\text{THF}$ gave the desired diborate **4** (eq 3). Chemical ionization mass spectrometry of **4** using NH_3 as the ionization gas gave a cluster of three large peaks at m/z 391, 392, and 393. This corresponds to the mass of **4** plus two ammonia molecules and a proton, and the observed relative intensities of m/z 391, 392, and 393 (0.50, 1.00, and 0.23) were in agreement with those calculated for a compound containing two borons (0.50, 1.08, and 0.21).

The X-ray crystal structure of **4** is shown in Figure 2. A symmetrical three-center two-electron $\text{B}\cdots\text{N}\cdots\text{B}$ bond is clearly absent from **4**. Rather, the molecule has acquired a molecule of THF (actually THF-*d*₈) at one boron, leaving the other boron to participate in an ordinary two-center two-electron B–N dative bond. Remarkably, the geometry of the “bottom” portion of **4** (i.e., that part containing the B–N bond) is virtually identical to that of **2** (see Table 2).

The 100 MHz ^{13}C NMR spectrum of **4** in THF-*d*₈ was examined at temperatures between room temperature and -90°C . The single line at 108.9 ppm (room temperature), due to C3 and C5, decoalesced as the temperature was lowered, becoming eventually two singlets of equal intensity separated by 513 Hz at -90°C . The small mystery mentioned above was thus resolved. A series of spectra taken at 1°C intervals near the coalescence temperature (T_c) enabled T_c to be determined as 262 ± 0.5 K. Therefore, ΔG^\ddagger at 262 K for the dynamic process which equilibrates C3 and C5 is 11.6 ± 0.1 kcal/mol.

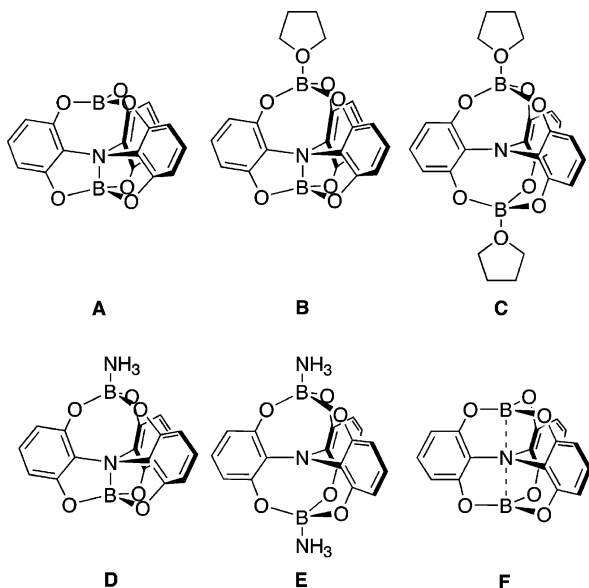
To help us understand the structure of **4** and its behavior in solution, ab initio calculations were performed on the structures shown in Chart 1. The choice of a basis set was a matter of concern, since the systems are unfortunately rather large. Performing calculations on smaller model systems seemed unwise, because in these systems there are bonding attractions or repulsions within the B–N–B triad itself, and there are forces on the B–N–B triad originating from the “outside”, i.e., from the conformational strains engendered by the “scaffold-

TABLE 2. Selected Structural Parameters of **4** and **2**^a

param	4	2 ^a	param	4	2 ^a
B(1)–N (Å)	1.683(4)	1.681(5)	Ph twist ^e (deg)	5.8(3)	3.1(9)
av C–N (Å)	1.460(3) ^b	1.470(18)	N–B(2) (Å)	2.959(4)	
av C–N–C (deg)	116.2(2) ^c	116.4(2)	av B(2)–O ^f (Å)	1.437(9)	
av O–B(1)–O (deg)	114.9(2)	114.4(3)	B(2)–O ^g (Å)	1.554(4)	
av O–B(1)–N (deg)	103.3(2)	103.9(3)	av C _{Ar} –O–B(2) (deg)	127.1(2)	
av B(1)–N–C (deg)	101.2(2)	101.1(2)	av O–B(2)–O ^f (deg)	115.5(7)	
av N–C–C ^d (deg)	109.9(2)	109.6(3)	av O–B(2)–O ^g (deg)	102.5(9)	
av C–C–O ^d (deg)	114.6(2)	115.7(3)	B(1)–N–B(2) (deg)	179.6(2)	

^a Reference 18a. ^b The average C–N lengths in **5** (ref 19) and **6** are 1.416(4) and 1.424(5) Å, respectively. ^c The average C–N–C angles in **5** (ref 19) and **6** are 120.0(2)° and 120.7(4)°, respectively. ^d The carbons are part of the N–B(1)–O–C–C five-membered ring. ^e In the N–B(1)–O–C–C five-membered ring, the “Ph twist” is the torsion angle between N–B(1) and C–C. ^f Endocyclic. ^g Exocyclic

CHART 1



ing”. The interplay between these two types of forces would be expected to be critical in describing the systems accurately. Therefore, paring down or eliminating phenyl rings, for example, was inadvisable, we thought. So, facing the necessity of tackling the full systems, we sought to economize as much as possible on the basis set. HF/3-21G* and B3LYP/3-21G* calculations on **2** gave B–N bond lengths of 1.823 and 1.775 Å, respectively, which agreed poorly with the experimental B–N length of 1.681(5) Å.^{18a} Although a larger basis set was called for, we felt the carbons and hydrogens did not need as extensive a basis as borons, nitrogen, and oxygens. Therefore, we used a 6-31G basis on carbons and hydrogens, and 6-31+G* on borons, nitrogen, and oxygens. We will denote this 6-31G(C,H);6-31+G*(B,N,O). A B3LYP/6-31G(C,H);6-31+G*(B,N,O) calculation on **2** gave a B–N bond length of 1.743 Å. In addition, we employed the LSDA/BP86/DN* method.

Table 3 shows the results of calculations performed on **A**. Of the four calculations, only HF/3-21G (entry 1) predicted a symmetrical B–N–B array. In the other cases, the symmetrical starting geometry desymmetrized, but only after many steps of geometry optimization. For example (entry 3), the starting symmetrical geometry changed very slightly in each of a very large number of optimization steps and then suddenly careened lower in energy by 4.1 kcal/mol to the final unsymmetrical

TABLE 3. Geometry of **A** Calculated by Various Methods

entry	method	B(1)–N (Å)	B(2)–N (Å)
1	HF/3-21G	2.332	2.336
2	B3LYP/3-21G*	1.843	2.654
3	LSDA/BP86/DN*	1.789	2.652
4	HF/6-31G(C,H);6-31+G*(B,N,O)	1.785	2.603
5	B3LYP/6-31G(C,H);6-31+G*(B,N,O)	1.766	2.635

B–N·····B geometry. The B3LYP calculation was extremely slow, oddly, and we abandoned this method.

Calculations on **B** (Table 4) show that the addition of THF to **A** is energetically favorable by 21 or 26 kcal/mol, which is consistent with the fact that **4** crystallizes as a THF adduct. The DFT calculation (entry 2) does a slightly better job at reproducing the experimental geometry of **4**·THF than the HF/6-31G(C,H);6-31+G*(B,N,O) method (entry 1). The NMR-detected degenerate equilibrium which **4**·THF undergoes in solution, which leads to time-averaged top/bottom symmetry, may be written in detail two ways, viz., eqs 5 and 6. Equation 5 is a dissociative pathway (loss of THF in the first step), and eq 6 is an

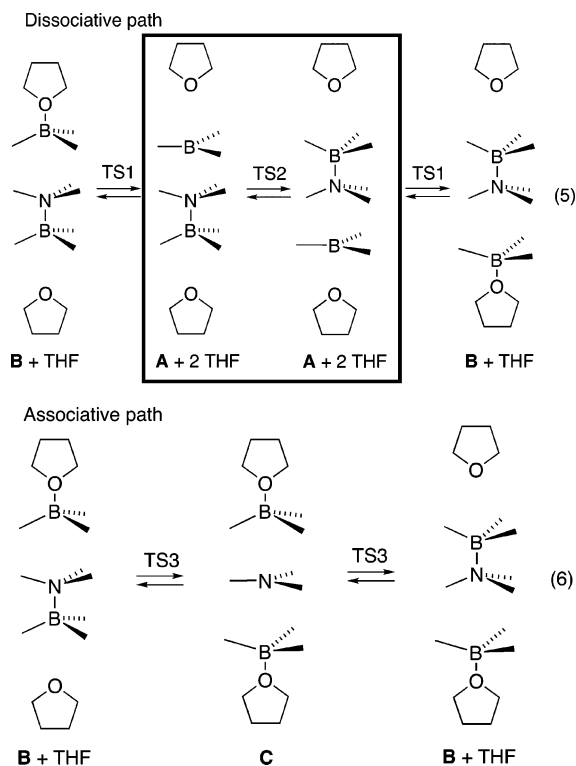


TABLE 4. Ab Initio Calculations on B–F

entry	species	method	E_{rel} (kcal/mol)	B(1)–N (Å)	B(2)–N (Å)
1	B	HF/6-31G(C,H);6-31+G*(B,N,O)	–21.25 ^a	1.739	2.911
2	B	LSDA/BP86/DN*	–26.21 ^a	1.717	2.965
3	4·THF	exptl ^b		1.683(4)	2.959(4)
4	C	HF/6-31G(C,H);6-31+G*(B,N,O)	+4.49 ^c	2.589	2.589
5	C	LSDA/BP86/DN*	+0.08 ^c	2.599	2.599
6	D	HF/6-31G(C,H);6-31+G*(B,N,O)	–27.35 ^d	1.745	2.908
7	E	HF/6-31G(C,H);6-31+G*(B,N,O)	–8.22 ^e	2.596	2.596
8	F	HF/6-31G(C,H);6-31+G*(B,N,O)	+2.66 ^f	2.261	2.262

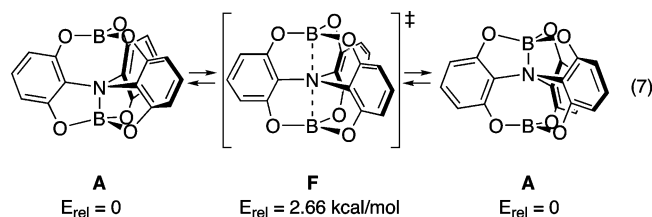
^a Relative to **A** + THF. ^b This work. ^c Relative to **B** + THF. ^d Relative to **A** + NH₃. ^e Relative to **D** + NH₃. ^f Relative to **A**; species **F** has one negative eigenvalue in the force constant matrix.

associative pathway (bonding to THF in the first step). For clarity, the equations omit the phenyls and most of the oxygens, i.e., the scaffolding.

In eq 5, the first step is the loss of THF from **B**, which is uphill in energy by 21 or 26 kcal/mol (Table 4, entries 1 and 2). This gives an estimate of part of the barrier to equilibration by the dissociative pathway. The Hammond postulate may be invoked for the highly endothermic dissociative step to argue that transition state TS1 will be close in energy to that of **A** + 2THF. An estimate of the energy of TS2 comes from the behavior of **A** during geometry optimization: the starting geometry (with a symmetrical B–N–B triad), which is a good approximation for TS2, was about 4 kcal/mol higher in energy than the optimized B–N·····B form. Thus, the dissociative path is calculated to have an overall barrier of at least 21 or 26 kcal/mol.

In eq 6, **C** lies 4.5 or 0.1 kcal/mol higher in energy than **B** + THF (Table 4, entries 4 and 5). Given the magnitude of this energy difference, it would be reasonable to assert that the barrier to equilibration by the associative path would be much lower than the minimum 21–26 kcal/mol calculated for the dissociative path. Therefore, the associative path, which includes no 3c-2e B–N–B bonding, seems more likely than the dissociative path, which does include 3c-2e bonding in TS2.

The generation of **4** in the presence of a Lewis basic solvent such as THF obviously affected the behavior of **4**. We have been unsuccessful in attempts to generate **4** in the absence of a Lewis base. Therefore, it was of great interest to quantify by calculation the energetics of the boxed part of eq 5 (a “bell clapper” mechanism²¹ of sorts). Species **F**, having a three-center two-electron bond, was confirmed as a transition structure (one imaginary frequency) lying 2.66 kcal/mol higher in energy than species **A** (eq 7). The B–N distances were 2.2612 and



2.2616 Å. The “phenyl twist” in **F** was found to be 8.2°; that is, **F** possessed very nearly C_3 symmetry. Another stationary point was found, having D_{3h} symmetry (B(1)–N

= B(2)–N = 2.2887 Å, phenyl twist 0°) 4.8 kcal/mol above **A**, but it was a second-order saddle point.

The calculation of a species such as **C** is formidable. To make the job slightly more tractable, we replaced the THF molecules in **B** and **C** with NH₃ molecules and did calculations on **D** and **E**. The addition of NH₃ to species **A** (Table 4, entry 6) was calculated to be favorable by 27.4 kcal/mol, as compared to 21.3 kcal/mol for addition of THF (entry 1). In contrast to the addition of a second THF to **B**, which is unfavorable by 4.5 kcal/mol (entry 4), addition of a second NH₃ to **D** to give **E** is favorable by 8.2 kcal/mol. This is consistent with the chemical ionization mass spectrometry results in which the major peak corresponds to an adduct of **4** with two NH₃ molecules plus H⁺, i.e., protonated **E**.

To summarize, **4** in the presence of THF does not engage in 3c-2e bonding. The 4·THF adduct is fluxional; the most likely pathway for degenerate equilibration does not involve 3c-2e bonding. Calculations suggest that, even if the complication of THF adduct formation were removed, **4** with a 3c-2e bond (**F**) would spontaneously distort to **A**.

The distortion is reminiscent of that found by BLS, whose all-carbon 3c-2e bond (**1b**) also was calculated to spontaneously distort.¹⁷ Transition structure **1b** relaxes by 14.1 kcal/mol, while transition structure **F** relaxes by 2.7 kcal/mol. Part of this difference is certainly due to differences in the basis set and other factors relating to the method of calculation, and the fact that **1** lacks phenyls, but some of the difference must reflect the change from an all-carbon system to a B–N–B system. Is the latter really more resistant than the former to distortion of the symmetrical triad? What factors affect the tendency of a linear X···Y···X system (a 3c-2e system) to distort to a linear X–Y·····X system? Would the same factors apply to in-line distortions of a 3c-4e system? Are 3c-4e systems intrinsically more resistant to in-line distortion than 3c-2e systems?

These questions may be addressed in terms of the second-order Jahn–Teller (SOJT) effect.²² Briefly, in this approach, a driving force for distortion of a symmetrical molecule exists if the direct product representation $\psi_{\text{HOMO}} \otimes \psi_{\text{LUMO}}$ of the undistorted molecule is the same as that of the symmetry coordinate which generates the distortion.

The general case of interest here has been treated previously.²³ The symmetries of the orbitals shown in

(21) Martin, J. C.; Basalay, R. J. *J. Am. Chem. Soc.* **1973**, *95*, 2572–2578.

(22) Nakatsuji, H.; Koga, T. In *The Force Concept in Chemistry*; Deb, B. M., Ed.; Van Nostrand Reinhold: New York, 1981; Chapter 3, pp 144–146.

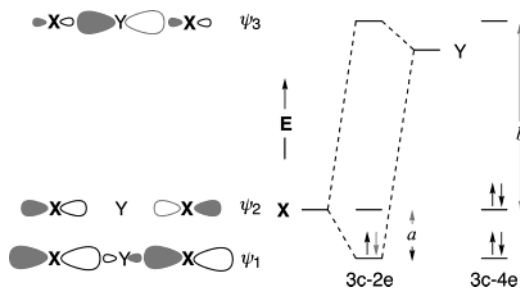


FIGURE 3. Three-center bond X–Y–X with X more electronegative than Y.

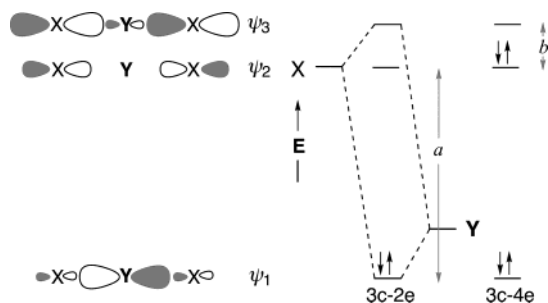


FIGURE 4. Three-center bond X–Y–X with X less electronegative than Y.

Figure 1 are ψ_1, σ_u^+ ; ψ_2, σ_g^+ ; and ψ_3, σ_u^+ . The symmetry coordinate leading to the in-line distortion ($X \cdots Y \cdots X \rightarrow X-Y \cdots X$, i.e., the asymmetric stretching mode) is σ_u^+ . In the 3c-4e case, the HOMO–LUMO ($\psi_2 \otimes \psi_3$) direct product is σ_u^+ , which is of the same symmetry as the asymmetric stretching mode. Thus, SOJT arguments predict that X–Y–X 3c-4e bonds prefer to be unsymmetrical. In the 3c-2e case, the HOMO–LUMO direct product is once again σ_u^+ (however, $\psi_1 \otimes \psi_2$ instead of $\psi_2 \otimes \psi_3$), so one reaches the same conclusion: X–Y–X 3c-2e bonds prefer to be unsymmetrical. For all symmetrical X–Y–X three-center bonds, 3c-2e or 3c-4e, there is a driving force toward the unsymmetrical triad, $X-Y \cdots X$.

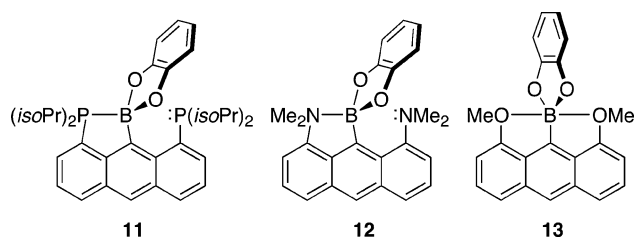
The *magnitude* of the driving force is inversely proportional to $E_{\text{HOMO}} - E_{\text{LUMO}}$.²² The orbital diagram of Figure 1 applies only if atom X is identical to atom Y. If, as is commonly the case, the terminal atoms X are more electronegative than the central atom Y, and therefore the p orbital of X is lower in energy than the p orbital of Y, the diagram will look like Figure 3. The energy gap “a” is the HOMO–LUMO separation in the 3c-2e case, and the energy gap “b” is the HOMO–LUMO separation in the 3c-4e case. If, on the other hand, the central atom is more electronegative (i.e., has a lower energy p orbital) than the terminal atoms, the orbital diagram will look like Figure 4, with a and b having the same meanings.

It is apparent on inspection of Figures 3 and 4 that the smallest HOMO–LUMO gaps, and therefore the largest driving forces for in-line distortion, are for (i) the two-electron case with termini more electronegative than the central atom (Figure 3, a) and (ii) the four-electron case with termini less electronegative than the central

atom (Figure 4, b). The systems *most resistant* to in-line distortion are (i) the two-electron case with termini less electronegative than the central atom (Figure 4, a) and (ii) the four-electron case with termini more electronegative than the central atom (Figure 3, b).

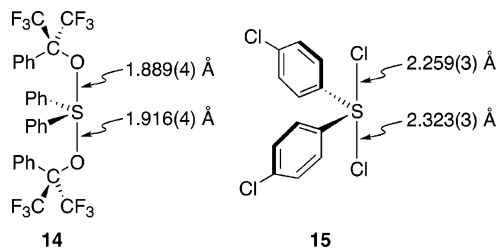
Both **1b** and **F** are 3c-2e systems. In these cases, SOJT arguments posit higher resistance to in-line distortion will result from increasing the difference in electronegativity between the central element and the terminal element, with the central element more electronegative than the termini. In **1b** there is no central–terminal electronegativity difference (all-carbon case), while for **F** the central nitrogen is more electronegative than the terminal borons. This should increase the resistance of **F** (relative to **1b**) to in-line distortion. Comparing our results ($\Delta E(\mathbf{F} \rightarrow \mathbf{A}) = -2.66$ kcal/mol) and those of BLS ($\Delta E(\mathbf{1b} \rightarrow \mathbf{1a}) = -14.1$ kcal/mol) yields a “trend” consistent with the SOJT argument, bearing in mind that the two results are not rigorously comparable, as mentioned before.

Support for the SOJT approach to the problem of in-line distortion in three-center bonds may be found in comparing the X-ray crystal structures of **11**,²⁴ **12**,²⁵ and **13**.^{8b} These are 3c-4e cases in which resistance to in-line



distortion should be increased by making the terminal elements increasingly more electronegative than the central element boron. In fact, **11** and **12** are “distorted” as shown, while **13**, with the most electronegative terminal element of the series, is symmetrical (Pauling electronegativities,²⁶ P, 2.1; N, 3.0; O, 3.5; p orbital energies²⁷ (eV), P, –9.52; N, –13.83; O, –16.76).

Three-center bonds which look symmetrical “on paper” often exhibit some distortion in their X-ray structures, e.g., **14**²⁸ and **15**.²⁹ Although structures such as these



(24) Yamashita, M.; Watanabe, K.; Yamamoto, Y.; Akiba, K.-y. *Chem. Lett.* **2001**, 1104–1105.

(25) Yamashita, M.; Kamura, K.; Yamamoto, Y.; Akiba, K.-y. *Chem.–Eur. J.* **2002**, *8*, 2976–2979.

(26) Pauling, L. *The Chemical Bond*; Cornell University: Ithaca, NY, 1967; p 64.

(27) Mann, J. B.; Meek, T. L.; Allen, L. C. *J. Am. Chem. Soc.* **2000**, *122*, 2780–2783.

(28) Paul, I. C.; Martin, J. C.; Perozzi, E. F. *J. Am. Chem. Soc.* **1972**, *94*, 5010–5017.

(29) Baenziger, N. C.; Buckles, R. E.; Maner, R. J.; Simpson, T. D. *J. Am. Chem. Soc.* **1969**, *91*, 5749–5755.

(23) (a) Burdett, J. K. *Molecular Shapes. Theoretical Models of Inorganic Stereochemistry*; Wiley: New York, 1980; p 86 ff. (b) Borden, W. T. *Theor. Chim. Acta* **1986**, *69*, 171–174.

have not been discussed in terms of SOJT distortion, the effect seems applicable in such cases. A confounding effect is the possibility of distortions caused by crystal packing forces on weak 3c-4e bonds.

Conclusions

The synthesis of diborate **4** made available for study a compound having a collinear BNB array and, thereby, the possibility of a 3-center 2-electron B··N··B bond. The fact that the immediate and penultimate precursors of **4** both have planar nitrogens seemed to increase the likelihood that **4** would also exhibit a planar (i.e., trigonal bipyramidal) nitrogen, and engage in 3c-2e bonding. The X-ray crystal structure revealed, however, no evidence for 3c-2e bonding (see Figure 2). A terminal boron was bonded externally to the oxygen of THF rather than internally to nitrogen. In THF solution, the nitrogen of **4** engages in a degenerate bond-switch equilibrium involving bonding of boron to THF. Calculations suggested that a bond-switch mechanism involving a 3c-2e B··N··B transition structure is unlikely. We conclude that it is unwise to employ a solvent capable of competing with the central element in bonding to the terminal atoms of a potential three-center bond. Although we tried a variety of ways to avoid THF (and any other Lewis basic solvents), we were unsuccessful in those attempts.

Calculations on “gas-phase” **4** showed that the form containing a symmetrical 3c-2e B··N··B array is a transition structure connected to, and 2.66 kcal/mol higher in energy than, the unsymmetrical 2c-2e B–N······B form.

Reasoning that it would be helpful for those designing new three-center (and more extended) systems to have some qualitative theoretical tool with which to predict or rationalize the occurrence of symmetrical versus unsymmetrical arrays, the SOJT approach to this problem was presented and applied to a few examples. The 3c-2e arrays (X··Y··X) most resistant to in-line distortion are those having central elements of high electronegativity and terminal elements of low electronegativity. The 3c-4e arrays most resistant to in-line distortions are those having central elements of low electronegativity and terminal elements of high electronegativity.

Experimental Section

Tris(2,6-dimethoxyphenyl)amine, 5.¹⁹ Under a nitrogen atmosphere, a mixture of 4.760 g (31.07 mmol) of freshly distilled 2,6-dimethoxyaniline (see the Supporting Information), 13.20 g (49.98 mmol) of 2,6-dimethoxyiodobenzene (see the Supporting Information), 36.40 g (263.4 mmol) of anhydrous powdered K₂CO₃, 8.474 g (133.4 mmol) of electrolytic copper, 1.842 g (6.969 mmol) of anhydrous 18-crown-6, and 60 mL of *o*-dichlorobenzene was brought to reflux. The progress of the reaction was monitored by silica gel TLC (5:1 hexanes/EtOAc). 2,6-Dimethoxyaniline and a reaction intermediate, bis(2,6-dimethoxyphenyl)amine, have nearly identical *R_f* values (0.7) but may be distinguished by the color generated by exposing the plate to iodine vapors. After 24 h, 2,6-dimethoxyiodobenzene and 2,6-dimethoxyaniline had both been consumed. The major species present was bis(2,6-dimethoxyphenyl)amine. (If desired, this product may be collected by silica gel column chromatography (hexanes/EtOAc, 5:1): mp 122–124 °C; ¹H NMR (250 MHz, CDCl₃) δ 6.75, (t, *J* = 8.1 Hz, 1H), 6.45 (d, *J* = 8.1 Hz, 2H), 5.47 (s, 1H), 3.61 (s, 12H); ¹³C NMR (63 MHz, CDCl₃) δ 151.5, 123.4, 119.9, 104.7, 57.0.

Anal. Calcd for C₁₆H₁₉NO₄: C, 66.42; H, 6.62; N, 4.84. Found: C, 66.33; H, 6.59; N, 4.77.) Additional 2,6-dimethoxyiodobenzene (8.800 g, 33.32 mmol) was added and the mixture refluxed 24 h longer. The TLC spot corresponding to **5** (*R_f* 0.4) was now the major spot. Silica gel column chromatography (hexanes/EtOAc, 5:1) gave a yellow solid, which was recrystallized from CH₂Cl₂/hexane to give 1.845 g (14.0% yield) of **5**: mp 190–1 °C (lit.¹⁹ mp 190–1 °C); ¹⁵N NMR (41 MHz, acetone-*d*₆) 57.2 (NH₃ reference).

Cyclization of 1,9-Dimethoxy-10-(2,6-dimethoxyphenyl)phenoxazine, 7. A mixture of 50 mg of **7** (0.13 mmol),¹⁹ 180 mg of copper powder (2.83 mmol), 760 mg of K₂CO₃ (5.50 mmol), and 36 mg of 18-crown-6 (0.14 mmol) in 3 mL of *o*-dichlorobenzene was heated at reflux under a nitrogen atmosphere for 10 days, at which time TLC (EtOAc/hexane, 1:3 (v/v)) showed two new spots at higher *R_f* than that of **7**. After silica gel chromatography, two fractions, A and B, were obtained. Data for fraction A (=9): 3 mg; FABMS *m/z* 288 (27, M + 1), 287 (100, M), 273 (22). ¹H NMR showed no discernible peaks, in either CDCl₃ or DMSO-*d*₆ solvent. Data for fraction B (=8): 8 mg; FABMS *m/z* 334 (31, M + 1), 333 (100, M), 287 (23); ¹H NMR (250 MHz, DMSO-*d*₆) δ 6.93 (apparent t, *J* = 8.2 Hz, 2H), 6.89 (dd, *J* = 8.9, 7.5 Hz, 1H), 6.75 (dd, *J* = 8.4, 1.3 Hz, 2H), 6.68 (d, *J* = 8.8 Hz, 1H), 6.68 (d, *J* = 7.6 Hz, 1H), 6.60 (dd, *J* = 8.1, 1.3 Hz, 2H), 3.59 (s, 6H); ¹³C NMR (63 MHz, DMSO-*d*₆) δ 150.7 (quat), 148.4 (quat), 146.3 (quat), 124.2 (CH), 124.0 (quat), 123.1 (CH), 120.1 (quat), 111.3 (CH), 108.9 (CH), 107.8 (CH), 55.7 (CH₃).

Tris(2,6-dihydroxyphenyl)amine, 6. To a stirred solution of 400 mg (0.944 mmol) of **5** in 30 mL of toluene, under rapid nitrogen purge, was added quickly 765 mg (5.74 mmol) of aluminum trichloride via one neck of the three-necked flask. The reaction mixture was quickly brought to reflux using an oil bath. The oil bath was turned off, and the flask and the oil bath were cooled together for 1.5 h. To the resulting green mixture was added 5 mL water, and stirring was continued for 15 min, at which time the mixture had become purple and deposited a lavender precipitate. This solid was collected by filtration, affording 300 mg (94% yield) of a material which was pure by ¹H and ¹³C NMR spectroscopy, albeit lavender. It was dissolved in 50 mL of boiling EtOAc, cooled, and extracted with 3 × 20 mL of 0.95 M NaOH. The basic extract was brought to pH 6 with 3 M HCl. The precipitate which resulted was taken up in 3 × 20 mL of EtOAc, and dried over Na₂SO₄. After decantation from the drying agent, the volume was reduced by half and stored overnight in the freezer, affording 155 mg (48% yield) of light pink crystals: mp 308–9 °C (discolors at 275 °C); ¹H NMR (250 MHz, THF-*d*₈) δ 8.12, (s, 6H), 6.69 (t, *J* = 8.1 Hz, 3H), 6.22 (d, *J* = 8.1 Hz, 6H); ¹³C NMR (63 MHz, THF-*d*₈) δ 157.3, 125.9, 123.5, 108.2; EIMS *m/z* 341 (M⁺), 244, 215, 198; IR (KBr) 3271, 2322, 1661, 1590, 1511, 1464, 1330, 1234, 1220, 1011, 791, 733 cm⁻¹.

A crystal, 0.44 × 0.44 × 0.06 mm, was chosen for X-ray crystallography, λ = 0.71073 Å; monoclinic, *a* = 14.092(5) Å, *b* = 8.590(2) Å, *c* = 21.856(6) Å, β = 94.64(2)°, *Z* = 4, space group *C2/c*. A total of 2433 reflections were collected (0 ≤ *h* ≤ +16, 0 ≤ *k* ≤ +10, -26 ≤ *l* ≤ +25; 2.78° ≤ θ ≤ 25.05°), 2332 of which were independent reflections (*R_{int}* = 0.0213). Solution and refinement by full-matrix least squares on *F²*, data-to-parameter ratio 13.2, gave a goodness of fit of 1.028, *R*₁ = 0.0658 and *wR*₂ = 0.1486 (*I* > 2σ(*I*)), and *R*₁ = 0.1205 and *wR*₂ = 0.1917 (all data). Crystalline **6** includes two molecules of ethyl acetate per molecule of **6**.

Tris(2,6-dihydroxyphenyl)amine Diborate, 4. To a solution of 10 mg (0.029 mmol) of **6** in 0.5 mL of THF-*d*₈ in a 5 mm NMR tube under nitrogen was added by syringe 0.0058 mL (0.058 mmol) of 1.0 M BH₃·THF. Gas was evolved over a period of 20 min, with warming to 36 °C in a water bath during the last 5 min. The reaction appeared quantitative by ¹H NMR: ¹H NMR (400 MHz, THF-*d*₈) δ 6.69 (t, *J* = 8.1 Hz, 3H), 6.22 (d, *J* = 8.1 Hz, 6H); ¹³C NMR spectral data given in Table 1; ¹¹B NMR (128 MHz, THF) δ 17.9. A sample of **4** prepared

as described spontaneously deposited crystals, which proved suitable for X-ray crystallography.

A crystal, $0.60 \times 0.32 \times 0.10$ mm, was chosen for X-ray crystallography, $\lambda = 0.71073$ Å: monoclinic, $a = 10.108(5)$ Å, $b = 14.080(6)$ Å, $c = 13.864(4)$ Å, $\beta = 92.89(4)^\circ$, $Z = 4$, space group $P2_1/n$. A total of 3700 reflections were collected ($-5 \leq h \leq +12$, $-10 \leq k \leq +16$, $-16 \leq l \leq +16$; $2.06^\circ \leq \theta \leq 25.05^\circ$), 3491 of which were independent reflections ($R_{\text{int}} = 0.0156$). Solution and refinement by full-matrix least squares on F^2 , data-to-parameter ratio 12.1, gave a goodness of fit of 1.016, $R1 = 0.0507$ and $wR2 = 0.1164$ ($I > 2\sigma(I)$), and $R1 = 0.0816$ and $wR2 = 0.1367$ (all data). Crystalline **4** includes one molecule of THF- d_8 per molecule of **4**.

Acknowledgment. We thank the Alabama Super-computer Center for generous allocations of time. Many

thanks are due to Dr. Dave Young for helpful discussions about the calculations and Prof. Robert A. Donnelly for unique insights with regard to the SOJT approach. The support of the Auburn University Chemistry Department is gratefully acknowledged.

Supporting Information Available: Experimental procedures for 2,6-dimethoxybenzamide, 2,6-dimethoxyaniline, and 2,6-dimethoxyiodobenzene, detailed results of calculations, spectroscopic data for **4–6**, **8**, and **9**, and X-ray crystallographic data, including ORTEP plots for **4** and **6** (PDF, CIF). This material is available free of charge via the Internet at <http://pubs.acs.org>.

JO0401990